

Article

Improved Design and Economic Estimation of Cold-End Systems for Inland Nuclear Power Plants

Wenjie Zhang¹, Yushan Li¹, Peiqi Liu²  and Huimin Wei^{2,*}¹ China Nuclear Power Engineering Co., Ltd., Beijing 100822, China² Key Laboratory of Power Station Energy Transfer Conversion and System, North China Electric Power University, Ministry of Education, Beijing 102206, China

* Correspondence: weihm@ncepu.edu.cn

Abstract: Reserve sites for coastal nuclear power plants are gradually being depleted, prompting a shift towards the development of inland nuclear power stations. A new cooling system based on the integration of multiple cooling sources using a hybrid dry–wet cycle is proposed to achieve a balance between energy and water consumption for inland nuclear power stations. Comparative studies among all the available cooling systems were further conducted to analyze the cooling performance and economic viability. The case study results indicate that, in comparison to relative humidity, the cooling performance and circulating water consumption of cooling systems are more susceptible to changes in dry-bulb temperature. In arid and water-scarce regions, a Combined Natural Draft Hybrid Cooling System generally exhibits a monthly average circulating water consumption rate that is more than 270 kg/s lower than that of the natural draft wet cooling system, with an average monthly back pressure reduction of 0.11 kPa. When the dry-bulb temperature exceeds 13 °C, the net profit of wet cooling surpasses that of hybrid cooling. However, this scenario undergoes a reversal as the dry-bulb temperature decreases and local water prices rise. It is emphasized that hybrid cooling demonstrates minimal impact when subjected to changes in environmental conditions, offering extensive regional applicability.

Keywords: natural draft hybrid cooling; inland nuclear plant; water/energy nexus; annual performance; economic analysis



Citation: Zhang, W.; Li, Y.; Liu, P.; Wei, H. Improved Design and Economic Estimation of Cold-End Systems for Inland Nuclear Power Plants. *Energies* **2024**, *17*, 2410. <https://doi.org/10.3390/en17102410>

Academic Editor: Sung Joong Kim

Received: 5 April 2024

Revised: 6 May 2024

Accepted: 10 May 2024

Published: 17 May 2024



Copyright: © 2024 by the authors. Licensee MDPI, Basel, Switzerland. This article is an open access article distributed under the terms and conditions of the Creative Commons Attribution (CC BY) license (<https://creativecommons.org/licenses/by/4.0/>).

1. Introduction

Unlike coastal nuclear power plants that use seawater as a cooling method, inland nuclear power systems are designed with ambient air and circulate fresh water as the cooling media. Currently, cooling systems are mainly classified into the following two categories: natural draft dry cooling system (NDDC) and natural draft wet cooling system (NDWC). NDDCs are widely used in water-scarce areas [1]. The heat exchange between air and water is achieved through the tower's heat exchanger. Since air and water do not come into direct contact, NDDC has almost no loss of circulating water. However, studies have shown [2] that the cooling capacity of NDDC towers sharply decreases when the environmental temperature is too high or when there is a crosswind. According to Du Preez and Kroger's [3] full-scale performance test results [4], the performance of horizontally arranged natural draft dry cooling systems is inhibited under the influence of environmental wind. Su [5] and Wang [6] studied the impact of environmental wind on the outlet of vertically arranged natural draft dry cooling systems using computational fluid dynamics (CFDs) [7], and the results showed that environmental wind had a "covering" effect on the tower's outlet, hindering the discharge of hot air. Wang [8] used a heat exchanger model based on the ϵ -NTU method and input the heat exchanger efficiency–wind speed curve. By monitoring the outlet water temperature of the heat exchange unit, the performance variation in the heat exchange system in winter was obtained. In addition, when the environmental temperature was too high or there was a high demand for

cooling performance [9], a spray cooling method for NDDC was proposed [10]. However, this method is hindered in low-temperature, high-humidity climates. The poor cooling performance and economic efficiency of NDDC limit its use in hot and humid regions.

NDWCs are widely used in regions with abundant water resources due to their simple structure [11], low cost, stable operation, and excellent cooling performance. In NDWC, water and air come into direct contact, and heat exchange occurs through the evaporation and cooling of water. The heat dissipation includes both heat and mass transfer, involving sensible and latent heat. Therefore, when the air temperature is high, the heat exchange capacity of NDWC is higher than that of NDDC [12]. However, there is a significant loss of circulating water through evaporation during operation [13], limiting the application of NDWC in water-scarce areas.

To date, a substantial number of researchers have conducted theoretical studies and simulation calculations on the key heat and mass transfer technologies of NDWC. Evaporation and convective heat transfer occur simultaneously at the air–water interface, and this heat and mass transfer system was initially described by Merkel [14]. However, Merkel made certain assumptions to simplify the calculations. Poppe et al. [15] considered strict differential equations for the enthalpy and humidity ratio of humid air with respect to water temperature, improving the Merkel model. The results indicated that the Poppe model's calculations were closer to the experimental results. In 2005, Kloppers [16] extensively discussed the heat and mass transfer equations of NDWC, derived the control equations for the Merkel model, ϵ -NTU model, and Poppe model, and used enthalpy–moisture curves to analyze the differences between the three models in the analysis and solution of cooling towers. Williamson [17] employed a two-dimensional axisymmetric numerical model to study the effects of changes in water spray density and fill thickness on the performance of cooling towers under uniform distribution. Al-Waked [18] pointed out, through a three-dimensional numerical model [19], that in real-world conditions, cooling towers were affected by crosswinds, disrupting the flow field inside the tower, deviating from the axisymmetric distribution under design conditions, resulting in a decline in cooling tower performance [20].

To achieve a balance between energy and water consumption in arid regions for nuclear power units, a scheme based on a combined dry–wet cycle hybrid cooling system is proposed. The aim is to address the cooling performance decline of NDDC in hot weather while simultaneously resolving the issue of excessive water consumption in NDWC [21].

To achieve adequate cooling performance with acceptable water consumption, an air-cooled heat exchange device can be added above the conventional wet cooling tower fill to construct a natural draft hybrid cooling system (NDHC). Currently, in addition to the theoretical research and numerical simulations of hybrid systems, there are few experimental studies and engineering application cases. Most research is focused on optimizing the operation and integration methods of hybrid systems. Huang [22] conducted theoretical research on the heat and mass transfer processes that occur when circulating water comes into direct contact with air in hybrid technology. It was observed that the introduction of a spray system inside NDDC could result in the obstruction of airflow, potentially leading to inferior performance compared to traditional dry cooling systems. Large droplet diameters and low spray water flow rates could deteriorate the heat exchange performance of the hybrid cooling method, even resulting in poorer heat exchange performance than traditional NDDC. Chen [23] performed a characteristic analysis of hybrid cooling towers based on the ϵ -NTU method, examining the applicability of hybrid systems in various meteorological environments. Wei [24] proposed an iterative algorithm to predict the performance of hybrid systems. This algorithm was applied in conjunction with the real operational parameters of a coal-fired power plant, considering the trade-off between water consumption and coal consumption. This study involved a comprehensive comparison and analysis of the performance and economic evaluations of the following three cooling systems: NDDC, NDWC, and NDHC.

The heat exchanger structure of the indirect air-cooling system is vertically placed at the bottom of the cooling tower, forming a cooling triangle. Two cooling columns are fixed on two sides of a triangular steel frame with an angle of approximately 50° , while the third side serves as the air passage. Air flows on the outside of the tube bundle, while the cooling water flows inside the tube bundle for cooling. The bottom of the cooling tower is equipped with louvers to regulate the airflow.

During the operation of a natural draft dry cooling system, there is a corresponding balance between the air extraction force and the resistance inside the tower.

$$\Delta p = \sum k_i \frac{\rho v^2}{2} \quad (1)$$

In a natural ventilation dry cooling system, heat dissipation primarily occurs through non-contact heat exchange between the air and water. This process involves the following three heat exchange modes:

1. Convective heat exchange between circulating water and the inner walls of the heat exchanger tubes.
2. Heat conduction from the inner walls to the outer walls.
3. Convective heat exchange between the outer walls of the heat exchanger tubes, fins, and other extended surfaces, and the surrounding air.

The heat exchanger tubes in NDDC are primarily composed of aluminum, which has excellent thermal conductivity. Therefore, the second part of the heat exchange, related to heat conduction, can be negligibly small. The convective heat exchange performance of the first and third parts is mainly associated with the structural design of the heat exchanger.

For the one-dimensional calculation model, this study adopted the classical logarithmic mean temperature difference method for computation. In the context of the first part of heat exchange, the classical Gnielinski formula [26] can be employed to calculate the heat transfer coefficient on the waterside.

$$Nu_w = \frac{\frac{f}{8}(Re_w - 1000)Pr}{1 + 12.7\sqrt{\frac{f}{8}}(Pr^{\frac{2}{3}} - 1)} \left[1 + \left(\frac{d}{L}\right)^{\frac{2}{3}} \right] \quad (2)$$

where f is the friction factor [27]

$$f = (1.82 \log_{10} Re_w - 1.64)^{-2} \quad (3)$$

The heat transfer coefficient on the waterside can be obtained from the finned tube bundle structure.

$$(h)_w = \frac{Nu_w \lambda_w}{d} \quad (4)$$

The heat transfer coefficient on the air side can be obtained as follows:

$$(h)_a = \frac{Q}{\frac{(T_w - T_{a,in}) - (T_w - T_{a,out})}{\ln \frac{T_w - T_{a,in}}{T_w - T_{a,out}}} A_a} \quad (5)$$

The total heat transfer coefficient of the heat exchanger can be calculated from the heat transfer coefficients of the water and air sides [28].

$$UA = \frac{1}{\frac{1}{(hA)_a} + \frac{1}{(hA)_w}} \quad (6)$$

By correcting the heat transfer temperature difference of the counterflow heat exchanger, corresponding to the inlet and outlet temperatures of the same cold and hot fluids, one can calculate the heat exchange of the NDDC heat exchanger.

$$Q = UAF_T \Delta T_{lm} = UAF_T \frac{(T_{w,in} - T_{a,out}) - (T_{w,out} - T_{a,in})}{\ln \frac{T_{w,in} - T_{a,out}}{T_{w,out} - T_{a,in}}} \quad (7)$$

The air moving from the outlet of the dry section to the outlet of NDDC undergoes an approximately adiabatic process. The pressure difference along the height is computed by the following formula:

$$p_{a4} - p_{a5} = p_{a4} \left(1 - 0.00975 \frac{h_5 - \frac{h_4}{2}}{T_{a4}} \right)^{3.5} \tag{8}$$

The expression for the loss coefficient of a cylindrical outlet is given by the following:

$$p_{a5} - p_{a6} = \left(0.02 Fr_D^{-1.5} - 0.14 Fr_D^{-1} \right)^{3.5} \left(\frac{m_a}{A_5} \right)^2 \frac{1}{\rho_{a5}} \tag{9}$$

where $Fr_D = \left(\frac{m_a}{A_6} \right)^2 \frac{1}{\rho_{a5}(\rho_{a5} - \rho_{a6})gd_5}$.

2.2. NDWC

The airflow in the NDWC is also driven by the density difference between the front and back of the fill, as shown in Figure 2.

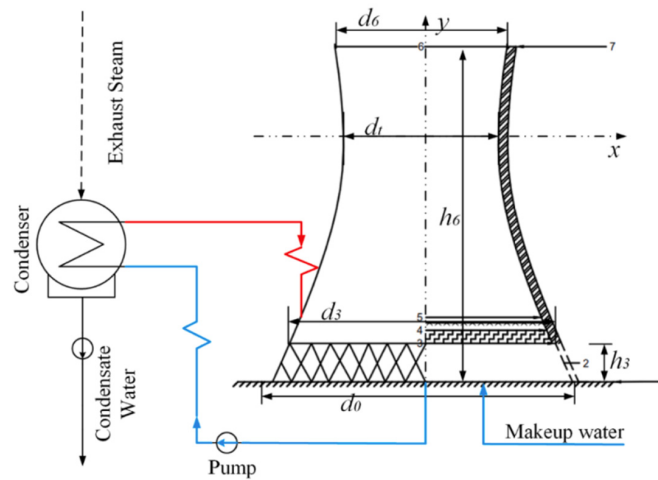


Figure 2. NDWC.

In NDWC, the circulating water is transported to the spray zone by the circulating water pump. The water is sprayed out from the nozzle, forming a diffused circular shape. The water then adheres to the fill and comes into direct contact with the air. Heat exchange occurs through the evaporation cooling of the water, and it finally drips down into the reservoir below.

For NDWC, it is necessary to consider the density variations in ambient air due to the absorption of water vapor.

$$\rho_{av} = (1 + w) \left(1 - \frac{w}{w + 0.62198} \right) \frac{p_a}{RT_a} \tag{10}$$

Unlike natural draft dry cooling systems, the process of moist air rising to the exit after passing through the fill in the tower is a typical pseudo-adiabatic process [29], and its temperature change can be expressed as follows:

$$\zeta_{T_{a5}} = \frac{-(1 + w_5) \left(1 + \frac{0.42216 \times 10^{-11} w_5^2 p_{a5} e^{\frac{5406.1915}{T_{a5}}} [h_{fgwo} - (c_{pw} - c_{pv})(T_{a5} - 273.15)]}{(w_5 + 0.62198) RT_{a5}} \right)}{c_{pma} + \frac{3.6693 \times 10^{-8} w_5^2 p_{a5} e^{\frac{5406.1915}{T_{a5}}} [h_{fgwo} - (c_{pw} - c_{pv})(T_{a5} - 273.15)]}{T_{a5}^2}} \tag{11}$$

Similarly, in the operation of NDWC, the air draft and resistance terms within the tower remain balanced; that is,

$$\Delta p = \sum k_i \frac{\rho v^2}{2} \quad (12)$$

The heat and mass transfer in the wet section of NDWC can be divided into three regions: the spray zone, the fill zone, and the rain zone. The heat and mass transfer in the rain zone is derived based on the Sherwood number of individual droplets [30]

$$\frac{h_{dr} a_{rz} H_i}{G_w} = 12 \left(\frac{D}{v_i d_d} \right) \times \left(\frac{H_i}{d_d} \right) \times \left(\frac{p_a}{R_v T_a} / \rho_w \right) \times \ln \left[\frac{w_s + 0.622}{w + 0.622} \right] (w_s - w) \times \int_0^{H_i} \int_0^{r_i} \left(\frac{v_i}{v_{dz}} \right) (2 + Sh) \left(\frac{r dr dz}{r_i^2 H_i} \right) \quad (13)$$

$$Sh = \frac{\beta d_d}{D} = 2 + 0.6 Re_d^{0.5} Sc^{0.33}$$

where Sh is the Sherwood number.

The heat exchange in the spray zone and fill zone can be calculated using Kröger's experimental relationships [31]

$$Me_{fi} = \frac{h_{d fi} a_{fi}}{G_w} L_{fi} = 0.25575 G_w^{-0.094} G_a^{0.6023} L_{fi} \quad (14)$$

$$Me_{sp} = \frac{h_{d sp} a_{sp}}{G_w} L_{sp} = 0.2 L_{sp} \left(\frac{G_a}{G_w} \right)^{0.5} \quad (15)$$

The Merkel number can be obtained by experiments as follows:

$$Me_{tot} = Me_{sp} + Me_{fi} + Me_{rz} \quad (16)$$

The Merkel number of the fill can be calculated by the Chebyshev four-point integration method [32].

$$Me_{tot} = \int_{T_{out,w}}^{T_{in,w}} \frac{c_{pw} dT_w}{i_{mas,w} - i_{ma}} = \frac{c_{pmw} (T_{in,w} - T_{out,w})}{4} \left(\frac{1}{\Delta i_{T=T_{out,w}+0.1(T_{in,w}-T_{out,w})}} + \frac{1}{\Delta i_{T=T_{out,w}+0.4(T_{in,w}-T_{out,w})}} + \frac{1}{\Delta i_{T=T_{out,w}+0.6(T_{in,w}-T_{out,w})}} + \frac{1}{\Delta i_{T=T_{out,w}+0.9(T_{in,w}-T_{out,w})}} \right) \quad (17)$$

The energy balance is calculated as follows:

$$Q_w = m_w c_{pmw} (T_{in,w} - T_{out,w}) = m_a (i_{mas,out} - i_{ma,in}) = Q_a \quad (18)$$

In contrast to NDDC, the ascent of humid air within the tower is considered a pseudo-adiabatic process.

$$p_{a34} - p_{a6} = p_{a5} \left[1 - \left(1 + \zeta_{Ta5} \frac{h_6 - h_3 - \frac{L_{fi}}{2}}{T_{a5}} \right)^{-\frac{0.021233(1+w_5)}{\zeta_{Ta5}(w_5+0.62198)}} \right] \quad (19)$$

$$p_{a6} - p_{a7} = \left(0.02 Fr_D^{-1.5} - 0.14 Fr_D^{-1} \right)^{3.5} \left(\frac{m_{av5}}{A_6} \right)^2 \frac{1}{\rho_{a6}} \quad (20)$$

where ζ_{Ta5} is the lapse rate and Fr_D is similar with NDDC.

2.3. NDHC

The NDHC is based on the parameters of the NDWC, with the addition of air-cooled tower fins for ultimate auxiliary cooling.

The proposed physical model of the NDHC is shown in Figure 3. The fill, a common component in the wet cooling section, is horizontally positioned above the tower support at the inlet height. The space above the fill and below the nozzles forms the spray zone. The heat exchanger, a typical component in the dry cooling section, is arranged vertically, surrounding the tower at elevation 6. Due to the density disparity between the interior

and exterior of the tower, air enters the tower simultaneously through the inlet at elevation 3 and the opening of the heat exchanger bundle at elevation 6, following a parallel-like trajectory. The air traverses through the fill, and the heat exchanger progresses along paths 2-3-4-5 and 6-7, converges at position 8, and proceeds outward to the environment at position 9. The water circulation on the waterside adopts a sequential arrangement, with circulating water passing through the heat exchanger, the spray zone, and the fill zone in sequence. Upon reaching the reservoir, it flows through valve V2, propelled by the circulation water pump, toward the condenser. By adjusting the valves, the flow direction of the circulating water can be modified, achieving the flexibility of changing between series and parallel operating modes. However, for the purposes of this study, only the series operating mode on the waterside was considered.

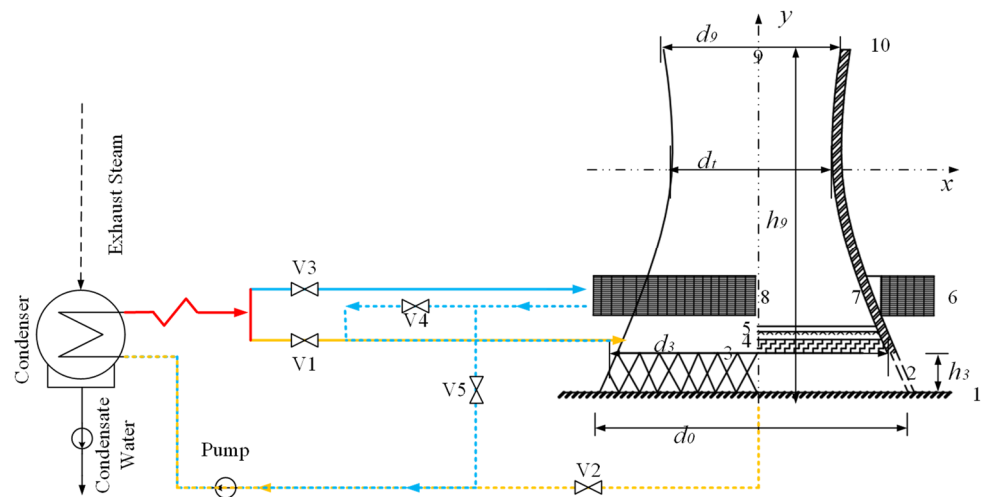


Figure 3. NDHC.

The calculations for the dry cooling section and wet cooling section are the same as the equations for standalone cooling towers discussed in previous sections. When air flows into the mixing section from two different regions, it can be considered based on mass-based averages.

$$m_{av8} = m_{a34}(1 + w_5) + m_{a67}(1 + w_7) \tag{21}$$

$$w_8 = \frac{w_5 m_{a34} + w_7 m_{a67}}{m_{a34} + m_{a67}} \tag{22}$$

$$h_{ma8} = \frac{h_{ma5} m_{a34} + h_{ma7} m_{a67}}{m_{a34} + m_{a67}} \tag{23}$$

The process from the mixing section to the system outlet can be described as follows [16]:

$$p_{a8} - p_{a12} = p_{a8} \left[1 - \left(1 + \zeta_{T_{a8}} \frac{h_9 - h_6}{T_{a8}} \right)^{-\frac{0.021233(1+w_8)}{\delta_{T_{a8}}(w_8+0.62198)}} \right] \tag{24}$$

2.4. Power-Generating Unit

Figure 4 illustrates the thermal power system diagram of an AP1000 unit with a rated power of 1250 MW at a nuclear power plant in China. The thermal power system comprises a steam generator, steam-water separation system, steam reheat system, turbine generator power system, high-pressure feedwater heating system, deaerator system, low-pressure feedwater heating system, condenser, and circulating water pump system, among others.

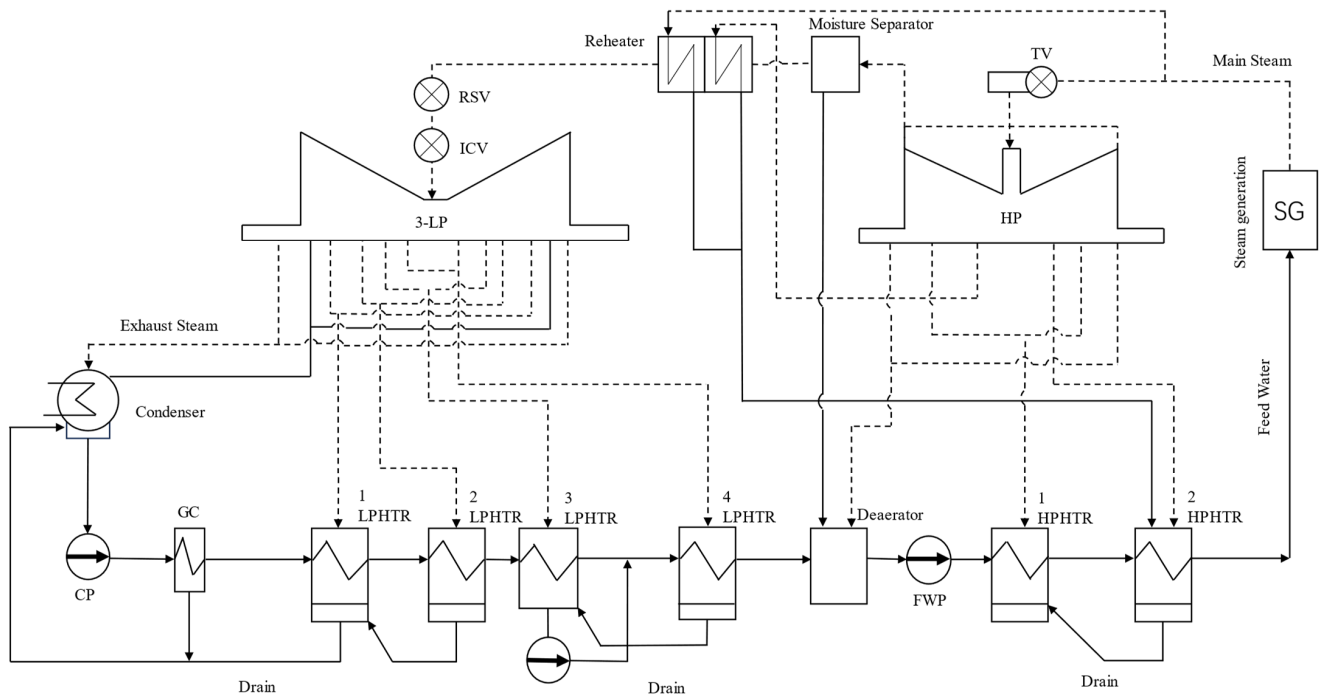


Figure 4. Schematic diagram of a nuclear power-generating unit.

The energy balance within the condenser can be expressed as follows:

$$Condenser \begin{cases} Q_s = M_c \Delta h_c \\ Q_h = (hA)_c \ln \frac{T_{in,w} - T_{out,w}}{T_s - T_{out,w}} \frac{T_s - T_{out,w}}{T_s - T_{in,w}} \end{cases} \quad (25)$$

The heat exchange performance within the condenser can be calculated using the empirical formulas provided by the Heat Exchange Institute (HEI) [33]

$$h_c = K_0 v_w \times K_W T_{out} \times F_M \times F_C \quad (26)$$

where K_0 , K_W , F_M , and F_C are correction factors.

The Flugel formula can be utilized to calculate the extraction pressures of each stage in the steam turbine under different back pressures [34],

$$\frac{M_i}{M_{i,0}} = \sqrt{\frac{P_i^2 - P_{i+1}^2}{P_{i,0}^2 - P_{i+1,0}^2}} \quad (27)$$

where M and P represent the mass flow rate and steam pressure of each stage, respectively.

The enthalpy value of extraction steam from the last stage of the steam turbine can be calculated based on the preceding stage. By fitting the efficiencies of individual stages under various operating conditions using a data-driven approach and storing the resulting models of stage efficiency as a function of stage flow in a database, one can predict the stage efficiency for any operating condition.

$$h_{2i} = h_{1i} - H_i \eta_i \quad (28)$$

By considering the heat exchange balance and mass conservation within each heater, the mass flow rate of extraction steam can be calculated as follows:

$$M_{es,j} = \frac{M_{fw,i} \tau_j - M_d \gamma_j}{q_j} \quad (29)$$

where M_{es} , M_{fw} , and M_d represent the mass flow rates of extraction steam, feedwater, and the drain, respectively. τ is the enthalpy rise of feedwater, while γ and q denote the heat output of drain and extraction steam, respectively.

The main flow of steam entering the high-pressure turbine of the steam turbine was successively reduced by the extraction steam flow from each stage, yielding the exhaust steam flow.

$$M_c = M_{ms} - \sum M_{es,j} \quad (30)$$

The power output of the unit can be determined based on the thermodynamic parameters of steam and the mass flow rate of extraction steam as follows:

$$P_e = \frac{M_c \Delta h_c + \sum M_{es,j} \Delta h_{es,j}}{\eta_m \eta_g} \quad (31)$$

Here, Δh_c and Δh_{es} represent the actual enthalpy drops of the exhaust steam and extraction steam, respectively. η_m and η_g , treated as constants, represent the mechanical efficiency of the generator and the electrical efficiency of power generation, respectively.

When the absolute value of the relative error between P_e and the design power load is less than 0.01%, it is considered that the values of the main steam mass flow rate and other operating parameters are relatively reasonable. Otherwise, the value of M_{ms} can be adjusted to repeat the calculations in Formulas (27)–(31) until the absolute value of the relative difference decreases to below 0.01%.

2.5. Cost Estimation

2.5.1. NDDC

The investment cost of a natural draft dry cooling system mainly consists of construction costs, operational costs, and maintenance costs. The construction costs are further divided into tower structure investment costs, heat exchanger investment costs, and circulation system investment costs. This section provides a simplified economic cost analysis, discussing the components and calculation methods of various costs [35]. The cost weighting factors used for subsequent cost calculations are uniformly presented in Table 1.

Table 1. Cost weighting factor.

Cost Weighting Factor	Symbol	Value
Construction		
Finned tube	W_{ft}	1.2
Header and frame	W_h	0.2
Heat exchanger bundle	W_{he}	1.2
Construction	W_c	1.25
Piping and valves	W_{pv}	0.25
Pump system	W_{ps}	1.25
Maintenance		
Heat exchanger bundle	W_{hem}	0.01
Structural	W_{cm}	0.0005
Pump system	W_{pm}	0.03
Piping and valves	W_{pvm}	0.005
Fill	W_{fi}	0.01

Heat exchanger bundle cost

1. Total finned tube cost per unit tube length, C_{ft} , CNY/m;

$$C_{ft} = (C_t + C_f + C_{sc})W_{ft} \quad (32)$$

where W_{ft} is the finned tube cost weighting factor; C_t is tube cost per unit tube length, ¥/m; C_f is the cost of fins per unit tube length, CNY/m; and C_{sc} is the surface coating cost per unit tube length, CNY/m.

2. Heat exchanger bundle header and frame cost, C_h , CNY/bundle;

$$C_h = C_{ft}L_t n_{tb}W_h \quad (33)$$

where W_h is the header and frame cost weighting factor; L_t represents the length of the finned tube, m; and n_{tb} represents the number of heat exchanger tube bundles.

3. Total finned tube cost per unit tube length, C_{he} , CNY/bundle;

$$C_{he} = (C_{ft}L_t n_{tb} + C_h + C_{ba})W_{he} \quad (34)$$

where W_{he} is the heat exchanger bundle cost weighting factor (installation); C_{ba} is the bundle assembly cost, CNY/bundle.

Natural draft cooling tower shell

1. Cost of land, excavation, and foundation, C_1 , ¥;

$$C_1 = C_{1u}A_b \quad (35)$$

where C_{1u} is the land, excavation, and foundation unit cost, CNY/m²; A_b is the tower base area, m².

2. Cost of the tower shell, C_{ct} , CNY;

$$C_{ct} = C_{ctc}V_{ts} \quad (36)$$

$$V_{ts} = 0.08333\pi(H_5 - H_t)(d_t^2 + d_t d_5 + d_5^2) + 0.08333\pi(H_t - H_3)(d_t^2 + d_t d_3 + d_3^2) \quad (37)$$

where C_{ctc} is the cost of the reinforced concrete used in the shell, CNY/m³; V_{ts} is the volume of reinforced concrete in the tower shell, m³. Subscript 5 represents the tower outlet, 3 represents the inlet, and t represents the throat.

3. Cost of the heat exchanger bundle platform, C_{hepl} , CNY;

$$C_{hepl} = C_{plu}A_{hepl} \quad (38)$$

where C_{plu} is the platform unit cost, CNY/m²; A_{hepl} is the heat exchanger platform area, m².

4. Cost of the tower supports, C_{ts} , CNY;

$$C_{ts} = C_{tsu}L_{ts}d_{ts}n_{ts} \quad (39)$$

where C_{tsu} is the tower support unit cost, CNY/m³; n_{ts} is the number of tower supports; d_{ts} is the diameter of tower support, m; and L_{ts} is the length of tower support, m.

5. Total construction cost, C_c , CNY;

$$C_c = (C_1 + C_{ct} + C_{hepl} + C_{ts})W_c \quad (40)$$

where W_c is the structural maintenance cost weighting factor.

Circulation system costs

1. Total pump system cost, C_{pst} , CNY;

$$C_{pst} = (C_{pump} + C_{em} + C_{ws})W_{ps} \quad (41)$$

where W_{ps} is the pump system cost weighting factor; C_{pump} is pump capital cost, CNY; C_{em} is electric motor cost, CNY; and C_{ws} is the electric wiring and switching cost, CNT.

2. Piping and valves cost, C_{pv} , CNY;

$$C_{pv} = n_{pump}C_{he}n_bW_{pv} \quad (42)$$

where W_{pv} is the piping and valves cost weighting factor; n_b is the number of bundles.

Operation cost estimation

1. Pump operating cost, C_{p0} , CNY;

$$C_{p0} = P_e C_{eav} \tau \quad (43)$$

where C_{eav} is the levelized electricity cost, CNY/kWh; P_e is the input power to the pumps, kW; and τ is the number of operating hours, h.

2. Fixed charges, C_{FCR} , ¥;

$$C_{FCR} = FCR \times C_{capital} \quad (44)$$

where $C_{capital}$ is the total capital cost, CNY; FCR is the levelized fixed charge rate.

Maintenance costs

The maintenance cost of the cooling system includes the heat exchanger, tower shell, pump system, and pipelines. The maintenance cost of different structures is equal to the construction cost of the structure multiplied by the maintenance cost weighting factor as follows:

$$\begin{cases} C_{hem} = W_{hem}C_{he} \\ C_{cm} = C_c W_{cm} \\ C_{pm} = C_{pst} W_{pm} \\ C_{pvm} = C_{pv} W_{pvm} \end{cases} \quad (45)$$

Total costs

The total annual cost of the cooling system is

$$C_{total} = C_{operating} + C_{maintenance} + C_{FCR} \quad (46)$$

The cost of power generation (attributed to the cooling system) is

$$C_{power} = \frac{C_{total}}{E_{net}} \quad (47)$$

2.5.2. NDWC

In the overall cost of tower construction, compared to air-cooled towers, NDWCs can reduce heat exchanger costs but increase filling material costs [36], as shown below

$$C_{fi} = V_{fi}C_{fic} \quad (48)$$

where the calculation method involves multiplying the volume of the fill material by the unit volume price.

In comparison to NDDC, the operational costs of NDWC also include the expenses related to the evaporative loss of circulating water, calculated as follows:

$$C_{evap} = m_{evap}C_{water} \quad (49)$$

where the calculation method involves multiplying the quantity of evaporated water by the local industrial water price.

In terms of maintenance costs, NDWCs lack the maintenance costs associated with heat exchangers but have additional maintenance costs related to filling materials.

3. Model Validation and Basic Data

In this chapter, commercial software MATLAB 2021a is utilized to develop the numerical models for the secondary and tertiary circuits of nuclear power plants. The cooling systems involved included NDDC, NDWC, and NDHC. To verify the accuracy of the models, design parameters from domestic engineering examples were referenced, and the simulation results were compared with actual operating data. For the NDHC, which lacks engineering precedents, the structural parameters were designed based on a similar back pressure to ensure that the condenser and turbine sides operated under similar conditions. This consistency helps to ensure that differences in performance in the comparative study are solely due to the type of cooling tower, allowing for a more accurate assessment of the performance differences among the various cooling towers, such as water consumption, environmental adaptability, and economic efficiency. In practical engineering applications, back pressure is an important design parameter for nuclear power plants. By adopting a consistent back pressure design, the research results have a better reference value for practical engineering applications.

3.1. NDWC

The NDWC references the Phase I Engineering Report of a 1250 MW nuclear power project in a certain location in southern China. The structural parameters are listed in Table 2. The designed back pressure for the power plant unit is 6.9 kPa.

Table 2. Design parameters of NDWC.

Parameter	NDWC
Tower height, m	223
Inlet height, m	17
Inlet diameter, m	154.39
Outlet diameter, m	97.36
Throat height, m	167.25
Throat diameter, m	93.086
Base diameter, m	169.05
Fill height, m	2
Circulating water flow rate, t/h	162,720
Inlet water temperature, °C	37.85
Spray area, m ²	18,000

The obtained heat transfer and outlet water temperature of NDWC through numerical simulations are shown in Table 3. As the model is based on the assumption of uniform inlet and outlet pressures, the heat transfer capacity may be slightly higher than the design value. However, this error is within an acceptable range for engineering purposes.

Table 3. Comparison between simulation results and design data of NDWC.

Parameter	Simulation Value	Design Value
Outlet water temperature, °C	25.52	25.72
Heat transfer, MW	2429.2	2243
Outlet air temperature, °C	32.8	32.25
Evaporation rate, kg/s	740	760
Air flow rate, kg/s	41,986.5	41,985.9

3.2. SNDDC

The structural data of the NDDC is referenced from an indirect air-cooled tower at a 1000 MW coal-fired power plant in Xinjiang, China. Its designed back pressure is 10 kPa, and the specific parameters are provided in Table 4.

Table 4. Design parameters of NDDC.

Parameter	NDDC
Tower height, m	195
Inlet height, m	31
Inlet diameter, m	124
Outlet diameter, m	94
Throat height, m	90
Throat diameter, m	94
Base diameter, m	151
Number of cooling triangles	164
Circulating water flow rate, t/h	79,344
Inlet water temperature, °C	41.74
Air cooled heat transfer area, m ²	2,220,000

Table 5 compares the simulated and design values of the heat transfer and outlet water temperature. After calculation, the error between the two is 0.88%, which is within an acceptable range. This indicates the reliability of the numerical simulation, supporting the subsequent application of the indirect air-cooled unit model from thermal power plants for the calculation and analysis of nuclear power air-cooled towers.

Table 5. Comparison between simulation results and design data of NDDC.

Parameter	Simulation Value	Design Value
Heat transfer, W	1.15×10^9	1.14×10^9
Outlet water temperature, K	302.45	302.5

Currently, there are no completed 1000 MW nuclear power indirect air-cooled units in China, and actual data are lacking. Therefore, only simulated air-cooled tower design parameters with a design back pressure close to the target are available for reference. By consulting the literature, characteristic data of AP1000 air-cooled turbines with varying back pressures were obtained [37]. Interpolating these data for a back pressure of 10 kPa, the simulated heat exchange capacity of a 1000 MW nuclear power indirect air-cooled tower was calculated to be 2408 MW. Through simulation, it was found that a single tower of the NDDC type used in thermal power plants would struggle to achieve such high heat exchange capacity. To achieve a heat exchange capacity of 2408 MW, the tower body parameters, heat exchanger parameters, and circulating water flow rate were increased. The calculated results indicated a tower height of 292 m and a circulating water flow rate of 170,000 t/h. Meanwhile, research showed that the largest cooling tower in the world was located at the Shengli Power Plant of the China National Energy Group. It has a tower height of 225 m. By comparison, the enlarged parameters of the million-level nuclear power indirect air-cooled tower already exceed those of the currently largest cooling tower in the world. In summary, the proposal to establish a single tower is not reliable, and future considerations should focus on the feasibility of a one-unit, two-tower scheme.

SNDDC arranges two NDDCs in series, with circulating water flowing successively through both NDDCs from the outlet of the condenser before finally returning to the condenser by the work of a circulating water pump, as shown in Figure 5. SNDDC ensures that the design back pressure is the same as that of the 1000 MW nuclear power indirect air-cooled tower, which is 10 kPa. For the convenience of design and calculation, the

parameters of the two serial NDDCs are selected to be consistent with specific design parameters, as shown in Table 6.

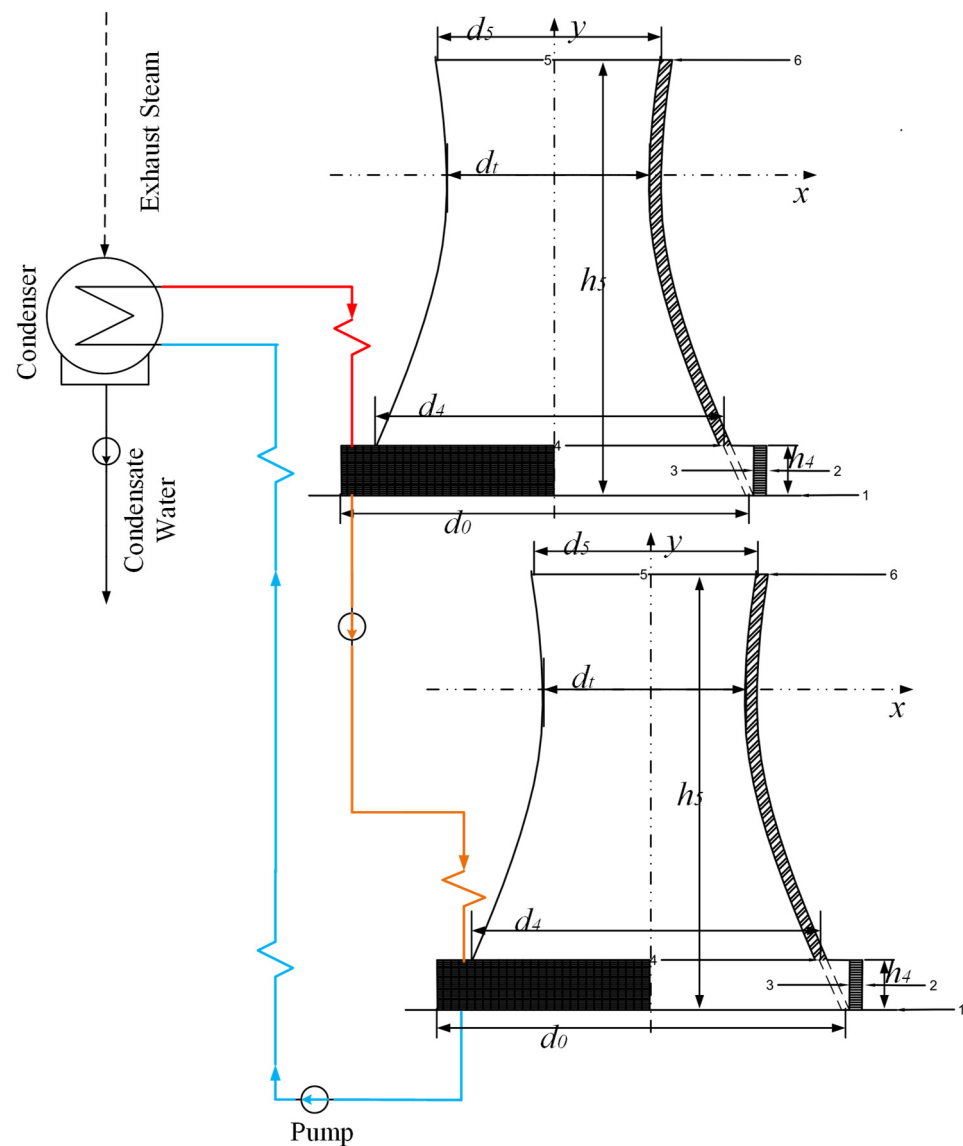


Figure 5. SNDDC.

Table 6. Design parameters of SNDDC.

Parameter	SNDDC
Tower height, m	213
Inlet height, m	33.9
Inlet diameter, m	144.5
Outlet diameter, m	109.6
Throat height, m	160.5
Throat diameter, m	104.9
Base diameter, m	176
Number of cooling triangles	212
Circulating water flow rate, t/h	170,000
Inlet water temperature, °C	41.74
Air cooled heat transfer area, m ²	2,840,000

3.3. CNDHC

CNDHC is based on the parameters of NDWC. It is positioned at a certain height above the wet cooling section, featuring vertically arranged heat exchangers encircling the tower.

The selection criteria for CNDHC are based on the same design of back pressure as NDWC. This means that under identical meteorological parameters, the total circulating water flow rate, inlet water temperature, and the outlet water temperature of the two tower types are kept consistent to ensure a uniform back pressure (6.9 kPa). Adjustments are made to the structural parameters of NDWC and NDDC, specifically to the tower body and heat exchanger parameters. The final results are presented in Table 7.

Table 7. Design parameters of CNDHC.

Parameter	CNDHC
Tower height, m	249
Inlet height of wet section, m	19
Inlet height of dry section, m	44.7
Inlet diameter, m	192.63
Outlet diameter, m	121.48
Throat height, m	186.8
Throat diameter, m	116.14
Base diameter, m	210.9
Fill height, m	2
Circulating water flow rate, t/h	162,720
Inlet water temperature, °C	37.85
Spray area, m ²	28,000
Number of cooling triangles	183
Air cooled heat transfer area, m ²	3,090,000

3.4. SNDHC

Figure 6 below is a schematic diagram of SNDHC. The circulating cooling water from the outlet of the condenser enters the heat exchanger of NDDC first, undergoing heat exchange through the work of the circulating water pump. It then enters the filling area of NDWC for cooling before returning to the condenser [38]. It is important to note that the outlet temperature of the circulating water in NDDC is equal to the inlet temperature of NDWC [39], and the outlet flow rate of the circulating water from NDDC is equal to the inlet flow rate of NDWC [40].

The structural parameters of SNDHC can be adjusted to ensure a back pressure of 6.9 kPa, with the structural parameters shown in Table 8.

Table 8. Design parameters of SNDHC.

Parameter	NDDC	NDWC
Tower height, m	204.75	205.16
Inlet height, m	32.55	15.64
Inlet diameter, m	130.2	142.04
Outlet diameter, m	98.7	89.57
Throat height, m	154.14	153.87
Throat diameter, m	94.5	85.64
Base diameter, m	158.55	155.53
Number of cooling triangles	164	/
Circulating water flow rate, t/h	164,000	164,000
Inlet water temperature, °C	37.85	37.85
Air cooled heat transfer area, m ²	2,450,000	/
Fill height, m	/	2
Spray area, m ²	/	15,478

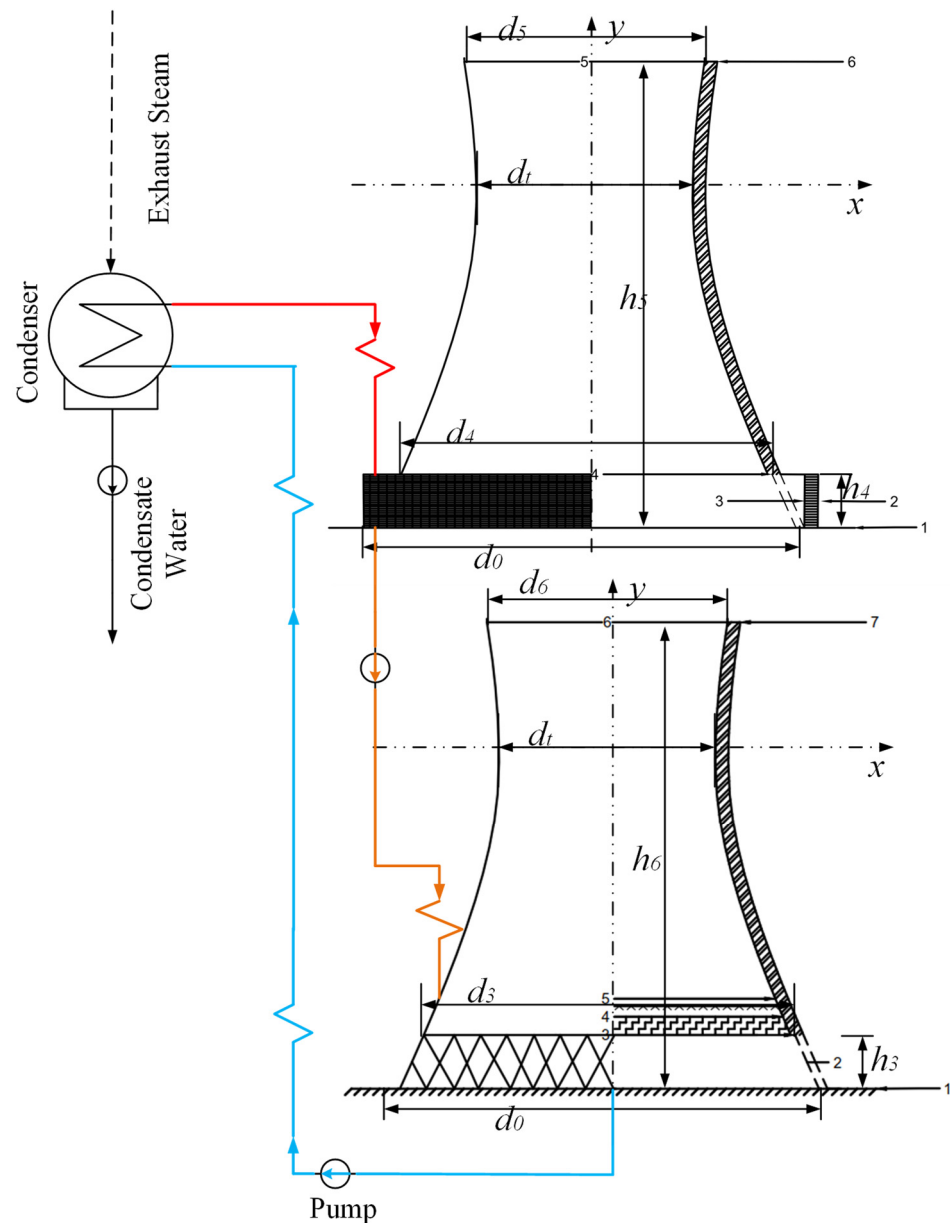


Figure 6. SNDHC.

3.5. Basic Data on the Plant Location

In China, the climate in the northern regions is mostly cold and dry, while the southern regions experience predominantly hot and humid conditions. To ensure representative site selection, one location from both northern and southern China was chosen. Guangdong Province, specifically Lianjiang City, was selected to represent the southern climate, while Shanxi Province, Jincheng City, Yangcheng County, was chosen to represent the northern climate.

A comparative study was conducted using the actual meteorological conditions in Yangcheng County, Jincheng City, Shanxi Province, and Lianjiang City, Guangdong Province. The monthly average meteorological parameters and the monthly operating hours of the power plants for Yangcheng County and Lianjiang City in 2018 are shown in Tables 9 and 10.

Table 9. The weather conditions in Yangcheng and the operational hours of the power plant.

Month	January	February	March	April	May	June
Ambient pressure, kPa	102.8	102.5	101.9	101.4	101.0	100.5
Ambient temperature, °C	−2.7	1.5	9.8	15.4	19.6	24.3
Ambient humidity, %	65.5	44.6	56.7	55.4	60.9	56.7
Operation hours, h	666.5	565.9	571.9	524.1	505.8	491.4
Month	July	August	September	October	November	December
Ambient pressure, kPa	103.5	105.5	101.5	102.2	102.5	103.0
Ambient temperature, °C	26.2	26.6	19.3	13.2	6.6	0.4
Ambient humidity, %	75.6	68.1	64.4	47.8	66.3	48.1
Operation hours, h	482.1	472.6	498.4	548.7	561.2	434.2

Table 10. The weather conditions in Lianjiang and the operational hours of the power plant.

Month	January	February	March	April	May	June
Ambient pressure, kPa	101.5	101.4	101.0	100.7	100.3	100.0
Ambient temperature, °C	16.7	17.3	21	24	27.6	29.1
Ambient humidity, %	81	85	89	87	85	82
Operation hours, h	666.1	565.6	571.6	523.8	505.6	491.2
Month	July	August	September	October	November	December
Ambient pressure, kPa	100.0	100.0	100.4	100.9	101.2	101.5
Ambient temperature, °C	28.9	28.3	27.8	25.2	22.4	17.2
Ambient humidity, %	83	85	83	78	80	73
Operation hours, h	481.8	472.3	498.1	548.4	560.9	434.0

For the purpose of economic analysis, the water and electricity prices for the two locations were found, as shown in Table 11.

Table 11. Water and electricity prices.

Location	Electricity Prices	Water Prices
Yangcheng	0.33 CNY/kWh	5.6 CNY/t
Lianjiang	0.43 CNY/kWh	3.2 CNY/t

4. Case Study with Discussion

This chapter explores the impact of various meteorological parameters on the performance of different cooling systems and analyzes the adaptability of these systems to the environment. The four cooling systems under discussion are NDWC (natural draft wet cooling systems), NDDC (natural draft dry cooling systems), CNDHC (Combined Natural Draft Hybrid Cooling Systems), and SNDHC (Separate Natural Draft Hybrid Cooling Systems). The operating parameters are uniformly set with a circulating water mass flow rate of 165,000 t/h and an inlet water temperature of 40 °C.

4.1. Sensitive Analysis under Different Ambient Conditions

Among numerous meteorological parameters, cooling towers are relatively sensitive to dry-bulb temperature and relative humidity. To investigate the sensitivity of different tower types to dry-bulb temperature and relative humidity and to encompass meteorological conditions in most regions of both northern and southern China, a range of dry-bulb temperatures from 5 °C to 35 °C, at intervals of 5 °C and relative humidity ranging from 20% to 80%, at intervals of 20%, were selected. Simulations were conducted to obtain the outlet water temperature and evaporation rate for different tower types, as presented in Table 12, where T_a is the dry-bulb temperature, RH is relative humidity, T_{out} is the outlet water temperature, and m_{evap} is evaporation.

Table 12. Sensitive analysis under different ambient temperatures and humidity.

RH, %	Ta, °C	T _{out} , °C				m _{evap} , kg/s		
		NDWC	SNDDC	CNDHC	SNDHC	NDWC	CNDHC	SNDHC
20	5	288.5	294.8	286.5	287.5	1299.6	767.7	759.0
	10	290.3	298.0	289.0	289.7	1299.8	818.5	813.9
	15	292.2	301.0	291.5	291.9	1281.2	850.8	857.2
	20	294.1	303.9	294.0	294.1	1239.3	859.7	886.9
	25	296.1	306.7	296.8	296.4	1175.3	828.3	897.7
	30	298.2	309.3	299.7	298.6	1082.2	757.0	887.7
	35	300.5	311.6	303.5	301.0	956.6	598.0	844.1
40	5	289.0	294.8	287.0	287.9	1246.0	712.0	714.0
	10	291.0	298.0	289.6	290.3	1231.4	750.6	754.6
	15	293.1	301.0	292.3	292.7	1194.3	768.0	783.0
	20	293.1	303.9	295.1	295.2	1132.6	760.9	792.5
	25	297.5	306.7	298.0	297.7	1043.6	719.1	781.5
	30	300.0	309.3	301.3	300.3	926.2	631.2	745.5
	35	302.7	311.6	305.3	303.1	775.6	463.7	672.3
60	5	289.5	294.8	287.5	288.4	1192.9	656.5	668.0
	10	291.7	298.0	290.3	291.0	1192.9	681.6	695.2
	15	293.9	301.0	293.1	293.6	1108.2	685.0	707.2
	20	296.4	303.9	296.1	296.3	1025.4	662.2	697.8
	25	299.0	306.7	299.3	299.1	912.8	604.4	665.1
	30	301.8	309.3	302.8	302.1	769.8	507.8	603.8
	35	304.9	311.6	306.9	305.2	594.7	336.1	507.3
80	5	290.0	294.8	288.0	288.9	1139.2	600.1	621.9
	10	292.3	298.0	290.9	291.6	1094.2	612.3	636.3
	15	294.8	301.0	294.0	294.4	1021.0	601.3	632.1
	20	297.5	303.9	297.2	297.4	917.8	563.0	603.8
	25	300.5	306.7	300.6	300.5	781.8	491.0	549.7
	30	303.7	309.3	304.3	303.8	614.9	382.6	464.1
	35	307.1	311.6	308.5	307.3	415.8	216.9	342.6
Average		296.05	303.61	296.04	295.93	/	/	/

In a cross-sectional comparison of data under identical meteorological parameters, circulating water flow rate, and inlet water temperature, it was observed that the SNDDC consistently exhibited the highest outlet water temperature, indicating its inferior heat exchange performance.

For the NDWC, it was noted that this type of tower consistently achieved the best cooling performance when the dry-bulb temperature exceeded 25 °C. However, when the dry-bulb temperature was below 25 °C, the CNDHC exhibited a superior cooling capacity among the four tower types.

For the SNDHC, a horizontal comparison revealed its excellent adaptability to changes in meteorological parameters. Although this type of cooling tower did not achieve the lowest outlet water temperature among the four types, the calculations indicate that the average outlet water temperature for the SNDHC was the lowest at 295.93 °C. In comparison, the average outlet water temperatures for the CNDHC and the NDWC were close, at 296.04 °C and 296.05 °C, respectively. Clearly, for a site with significant variations in meteorological conditions, the SNDHC exhibited optimal heat exchange performance.

In a vertical comparison of each column of data, due to the absence of direct contact between the air and water during the internal heat exchange process in the SNDDC, changes in humidity in the environment did not affect the heat and mass transfer in SNDDC. For the other three tower types, it was observed that as the relative humidity increased, the heat exchange performance of the cooling towers significantly decreased. This phenomenon is attributed to the fact that all three tower types have a filled part, and the heat exchange

of circulating water in the filling primarily depends on the evaporative cooling process, which is weakened by higher relative humidity.

As the dry-bulb temperature increases, the heat exchange capacity of all four tower types decreases. This is because the cooling principle of cooling towers relies on the heat exchange between circulating water and ambient air to achieve a reduction in water temperature. When the temperature difference between the air and circulating water decreases, the heat exchange performance correspondingly deteriorates.

In terms of evaporation, it is observed that the evaporation rate of NDWC is consistently the highest under any meteorological condition. This is attributed to the fact that, compared to the other two tower types, NDWCs only have the wet section in their heat exchange structure, while SNDHC and CNDHC also provide a dry section heat exchanger for additional heat exchange. When comparing these two hybrid tower types, it was found that the evaporation rate of CNDHC is always superior to that of SNDHC. The advantage becomes more pronounced with higher dry-bulb temperatures. At a dry-bulb temperature of 35 °C and a relative humidity of 20%, the maximum difference in evaporation rates between the two is 246.1 kg/s.

In a vertical comparison of evaporation rates for each column, it was observed that higher relative humidity and higher dry-bulb temperatures correspond to lower evaporation rates. This is because an increase in relative humidity weakens the evaporative cooling process, while an increase in dry-bulb temperature reduces the ventilation rate inside the tower.

The regression curve obtained for the non-standardized outlet water temperature is given as follows, reflecting the multivariate linear relationship. This regression curve provides insights into the impact of unit changes in meteorological parameters on the outlet water temperature and evaporation rate. The results indicate that in the linear regression curve for NDWC, the coefficient for relative humidity is the largest at 0.06343. This suggests that changes in relative humidity have the greatest impact on the cooling performance of NDWC when measured in unit increments. However, changes in dry-bulb temperature have the smallest impact on the outlet water temperature of NDWC. The CNDHC outlet water temperature was found to be most influenced by changes in dry-bulb temperature but less susceptible to changes in relative humidity. SNDHC fell between the two, indicating the best adaptability to environmental changes. This result aligns with the earlier analysis.

$$\begin{cases} T_{NDWC} = 283.22 + 0.06343R_H + 0.48304T_a \\ T_{CNDHC} = 292.37 - 1.15 \times 10^{-15}R_H + 0.56214T_a \\ T_{SNDHC} = 282.36 + 0.059R_H + 0.53071T_a \end{cases} \quad (50)$$

The non-standardized multivariate linear regression curve for the evaporation rate is presented below. The results indicate that the evaporation rate of NDWC is most susceptible to unit changes in dry-bulb temperature and relative humidity. The coefficient for dry-bulb temperature (T_a) is notably high at 17.86, surpassing the dry-bulb temperature coefficient for NDHC by a considerable margin. This suggests that NDHC is effective at achieving water conservation goals.

$$\begin{cases} m_{NDWC} = 1661.58 - 5.59R_H - 17.86T_a \\ m_{CNDHC} = 1049.73 - 4.79R_H - 8.56T_a \\ m_{SNDHC} = 1008.75 - 4.99R_H - 2.99T_a \end{cases} \quad (51)$$

The non-standardized regression curves mentioned above provide insights into the adaptability of different cooling systems to fluctuations in environmental parameters. To assess the sensitivity of different cooling systems to environmental parameters, it is necessary to dimensionless the data and obtain standardized multivariate linear regression curves. The calculated results are as follows.

Analyzing the sensitivity of different cooling systems to environmental variables, the results indicate that, compared to NDWC, NDHC exhibits lower sensitivity to relative humidity but higher sensitivity to dry-bulb temperature in terms of cooling performance. In contrast to NDWC, NDHC shows lower sensitivity of evaporation rates to dry-bulb temperature but higher sensitivity to relative humidity.

$$\begin{cases} T_{NDWC} = 56.9721 + 0.2779R_H + 0.9466T_a \\ T_{CNDDC} = 52.9717 + 0 \times R_H + 0.9988T_a \\ T_{CNDHC} = 45.966 + 0.1892R_H + 0.9769T_a \\ T_{SNDHC} = 52.7828 + 0.2396R_H + 0.9640T_a \end{cases} \quad (52)$$

$$\begin{cases} m_{NDWC} = 4.4162 - 0.5473R_H - 0.7803T_a \\ m_{CNDDC} = 4.0538 - 0.6926R_H - 0.5534T_a \\ m_{SNDHC} = 5.2570 - 0.8541R_H - 0.2287T_a \end{cases} \quad (53)$$

4.2. Thermal Performance of Cooling Systems

The simulated heat exchange capacities of different cooling systems in Yangcheng and Lianjiang are illustrated in Figure 7, where hollow symbols represent Lianjiang, while solid symbols represent Yangcheng. The image on the right is an enlarged view of the black dashed box in the left image. It can be observed that, regardless of the geographical location (north or south), SNDDC consistently exhibits the lowest heat exchange capacity among the four tower types. For the other three tower types, which are designed with the same back pressure, the differences in heat exchange capacity are not pronounced. However, upon closer inspection, it is evident that during colder months, CNDHC has the highest heat exchange capacity, while NDWC has the lowest. As temperatures rise, the heat exchange capacity of NDWC gradually surpasses that of the hybrid systems, aligning with the conclusions drawn in the sensitivity analysis section.

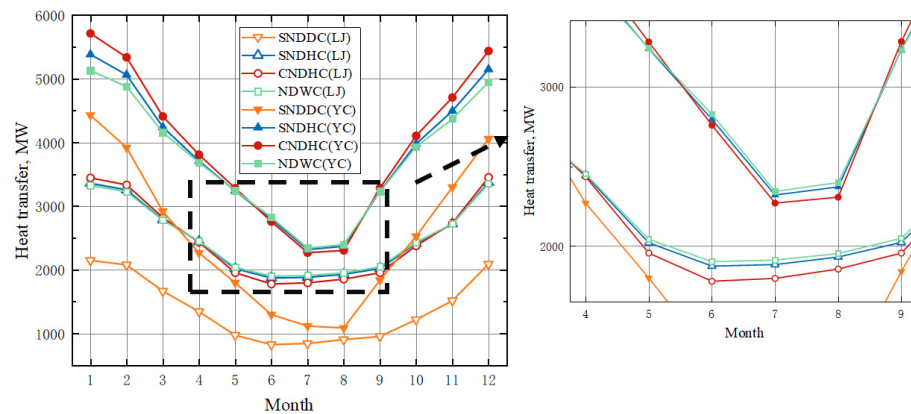


Figure 7. Monthly cooling performances of different cooling systems.

To compare the heat exchange performance of the dry and wet sections in hybrid systems, the heat exchange capacity of the dry and wet sections of hybrid systems under the climatic conditions in Yangcheng is shown in Figure 8. In this context, CNDDC consists of two NDDC units connected in series; hence, the heat exchange capacity of the two dry sections is presented. It was observed that in the hybrid systems, the efficiency of the dry section is relatively low because the dry section primarily transfers sensible heat, with the majority of the heat exchange occurring in the wet section. However, under relatively colder climatic conditions, the gap in heat exchange between the dry and wet sections of hybrid towers gradually diminishes. In January and December, the heat exchange in the dry section of CNDHC even surpasses that of the wet section.

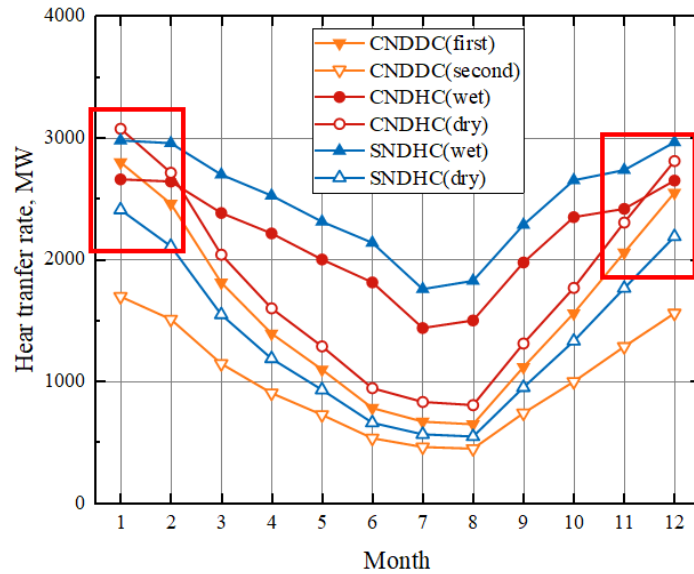


Figure 8. Heat exchange in different sections of the hybrid system.

When the reference temperature is 263.15 K, the enthalpy values of saturated moist air vary with air temperature [25], as shown in Figure 9. The curves of sensible heat and latent heat intersect, indicating that, at relatively low temperatures, the sensible heat of pure dry cooling exceeds the latent heat of pure wet cooling. When the ambient temperature is low, the corresponding saturated moist air state parameters have a limited capacity to absorb water vapor, and the low evaporation rate on the circulating waterside results in saturation. At this point, the higher ventilation rate of the natural draft dry cooling system allowed it to surpass the heat exchange capacity of NDWC under conditions of lower dry-bulb temperatures. Generally, such meteorological conditions are uncommon in Australia and Africa, where natural draft dry cooling systems are more commonly adopted and, thus, are infrequently reported.

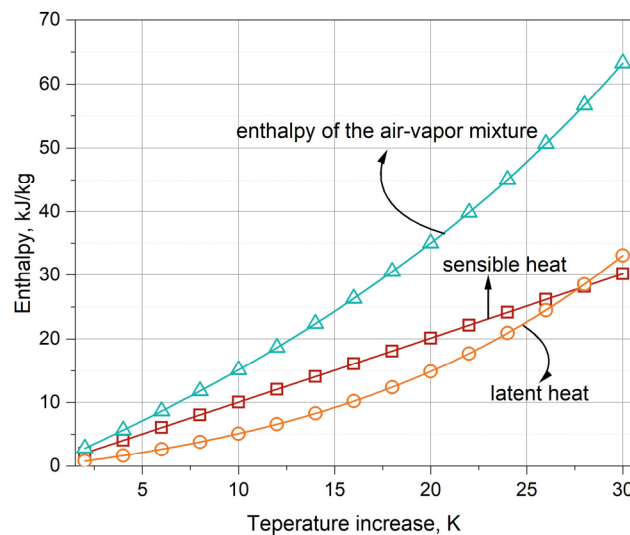


Figure 9. Enthalpy variations in the air–vapor mixture with the increase in air temperature.

4.3. Comparative Analysis of Back Pressure

Based on the established coupled model of the nuclear power plant’s secondary circuit and the cooling tower, the monthly variation in back pressure for the power plant was calculated, as illustrated in Figure 10. The image on the right is an enlarged view of certain curves from the image on the left. As analyzed in Section 4.2 earlier, under sufficiently cold

meteorological conditions, the heat exchange capacity of air cooling could even surpass that of wet cooling, as seen in the meteorological parameters for Yangcheng in January. When the dry-bulb temperature was -4 degrees Celsius, the back pressure of SNDDC was already lower than that of NDWC.

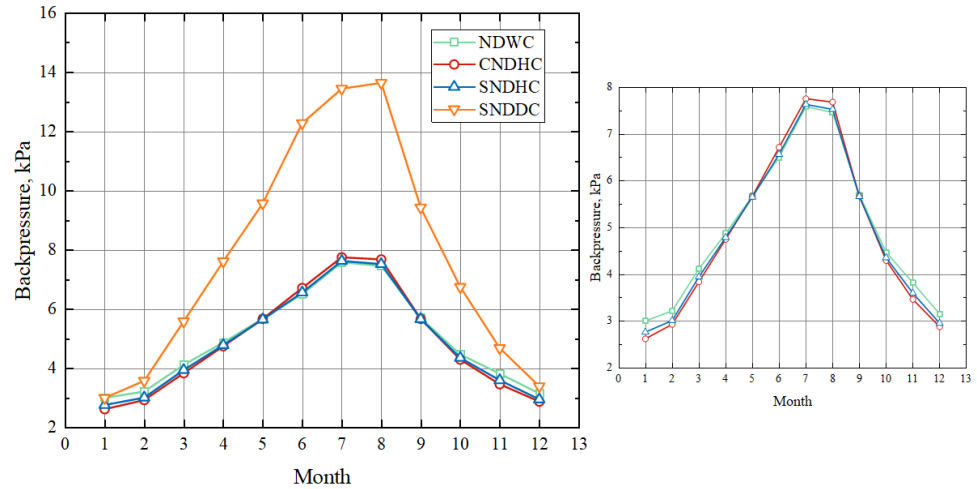


Figure 10. Annual back pressure variations in the power-generating unit coupled with different cooling systems in Yangcheng.

The right chart depicts the image with the SNDDC curve omitted. It can be observed that approximately in May and September, under the environmental conditions of Yangcheng, the three curves intersect. When the temperature is below these two months, NDWC exhibits the highest back pressure, and CNDHC has the lowest back pressure. Moreover, the difference in back pressure between the two increases as the temperature decreases, reaching 0.25 kPa in January. When the temperature exceeds that of May and September, the back pressure of the hybrid system gradually surpasses that of NDWC. The maximum difference in back pressure occurs in August, reaching only 0.06 kPa.

The following Figure 11 illustrates the variation in back pressure for different tower types in Lianjiang. The image on the right is an enlarged view of certain curves from the image on the left. The right chart presents the image with SNDDC excluded, showing a similar relative size relationship in back pressure, as observed in Yangcheng. For low temperatures, the hybrid system is more favorable, while the NDWC is more advantageous in high temperatures. The maximum back pressure difference between the CNDHC and NDWC in the summer occurs in June, amounting to 0.09 kPa. Thus, the advantage of the CNDHC is evident in low-temperature climates, with the potential for a back pressure reduction of 0.25 kPa compared to NDWC. Even in the summer climate of the southern region, the back pressure difference is within the range of 0.09 kPa, further emphasizing the cooling potential of the hybrid system.

It can be observed that, whether in Yangcheng or Lianjiang, the unit back pressure is high in summer and low in winter. When the cooling system is coupled with the nuclear power unit, the cooling system's inlet water temperature decreases with the ambient temperature. A higher heat exchange performance ensures lower system back pressure and higher power generation. The increase in power generation allows the nuclear power unit to produce more electricity in the same period, generating higher revenue. However, the operating cost of the unit is also an important factor to consider when calculating economic feasibility. The subsequent analysis involves a comparative analysis of the operating costs of the cooling systems.

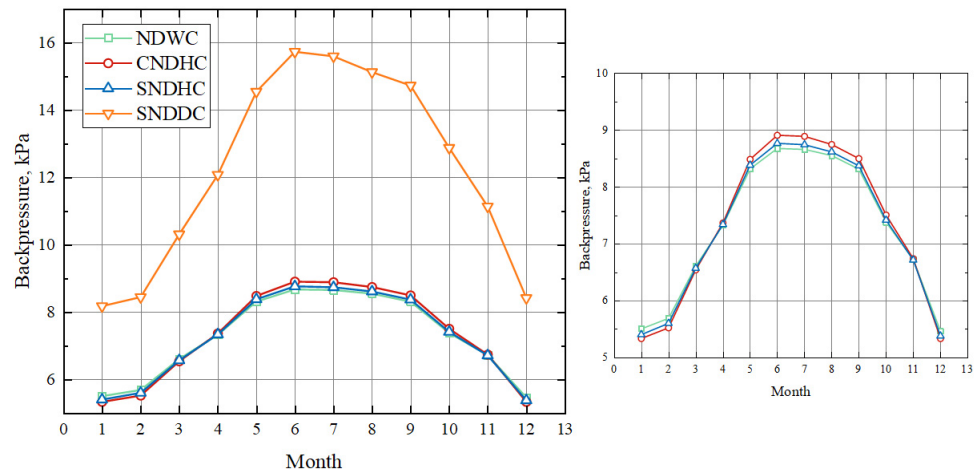


Figure 11. Annual back pressure variations in the power-generating unit coupled with different cooling systems in Lianjiang.

4.4. Water Consuming

NDDCs are more popular in the northern regions due to their excellent water-saving performance. Among the operating costs of cooling towers, the cost of makeup water is significant. Excellent water-saving performances can significantly reduce later operational expenses. In this section, we conduct a comparative analysis of the water-saving performance of the four tower types in plant locations in both northern and southern regions.

The following Figures 12 and 13 depict the variation in evaporation for the cooling systems in Yangcheng and Lianjiang, respectively. The order of evaporation from high to low is NDWC, SNDHC, CNDHC, and SNDDC. In the climate of Yangcheng, the average monthly cycle water evaporation rate of SNDHC is 200 kg/s lower than that of NDWC, and the evaporation rate of CNDHC is 270 kg/s lower than that of NDWC. In the climate conditions of Lianjiang, the average monthly cycle water evaporation rate of SNDHC is 190 kg/s lower than that of NDWC, and CNDHC is 276 kg/s lower than NDWC. In Yangcheng, the evaporation sharply decreases from June to July, which is attributed to the increase in relative humidity from 56.7% to 75.6%.

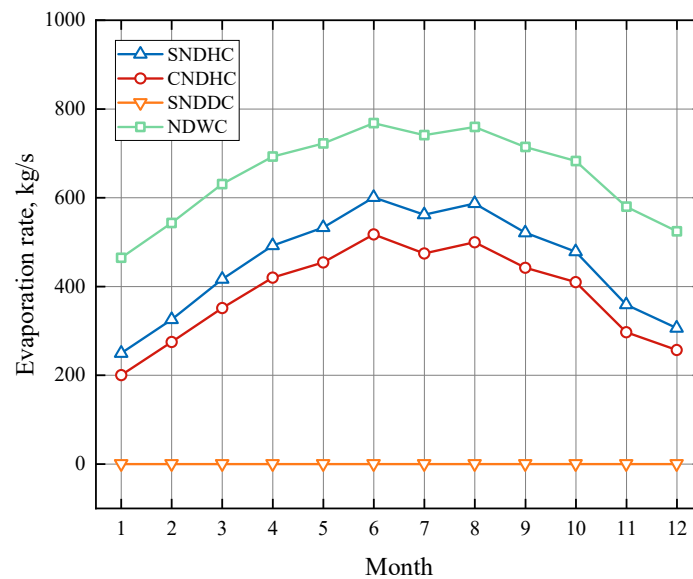


Figure 12. Annual water consumption rate in Yangcheng.

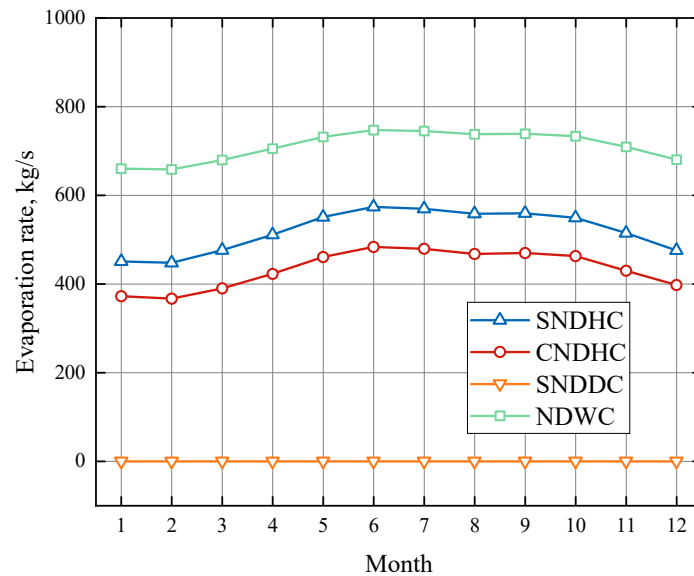


Figure 13. Annual water consumption rate in Lianjiang.

The NDWC exhibits the highest evaporation volume as it relies primarily on the evaporative cooling of the fill, while the hybrid cooling system incorporates both wet and dry sections to achieve water saving. SNDDC has minimal water evaporation losses due to the air-cooling heat exchanger. Excluding SNDDC, CNDHC has the lowest evaporation volume. The subsequent optimization of the operational mode by adjusting the flow rates to the dry and wet sections could further reduce operating costs and increase net profit.

It is worth mentioning that the conclusion in the earlier Section 4.1 was that the evaporation of the cooling system can decrease in hot and humid climates. This is in direct contrast to the conclusion in this section. The reason for this discrepancy is that, when coupled with the power generation unit, more water is required for heat exchange in hot summers to ensure that the unit can achieve a lower back pressure.

4.5. Operation Cost

The total operating costs mainly include the costs of pump operation and the cost of circulating water evaporation losses. Figure 14 depicts the variation in operating costs for different cooling systems in Yangcheng. The order from high to low is NDWC, SNDHC, CNDHC, and SNDDC. SNDHC has an average monthly operating cost of CNY 48 million lower than NDWC, and CNDHC has a cost of CNY 66 million lower than NDWC.

Due to the small tower parameters and fewer pump units, NDWC has the minimum pump operation cost, but it also has the highest rate of circulating water evaporation, and evidently, the low cost of pump operation cannot compensate for the losses caused by circulating water evaporation. SNDDC incurs no consumption of circulating water, resulting in the lowest operating cost.

It is worth noting that in the summer, the operating cost gap between the NDWC and hybrid system narrows while it widens during cold weather. The difference reaches its maximum in January, and the sudden drop in operating costs in December is due to the lowest monthly operating hours.

Due to the humid climate conditions in Lianjiang, compared to Yangcheng, the evaporative losses of circulating water for various cooling systems decreased. Coupled with the lower industrial water prices in the southern region, the difference in circulating water consumption costs among different cooling systems decreased. As a result, the proportion of circulating water consumption costs in the total operating costs decreased, while the proportion of pump operation costs increased. At this point, the operating costs of NDWC were lower than those of NDHC, as shown in Figure 15. Clearly, in the humid climate of

the southern region and with lower industrial water prices, water-saving cooling systems struggle to demonstrate their advantages.

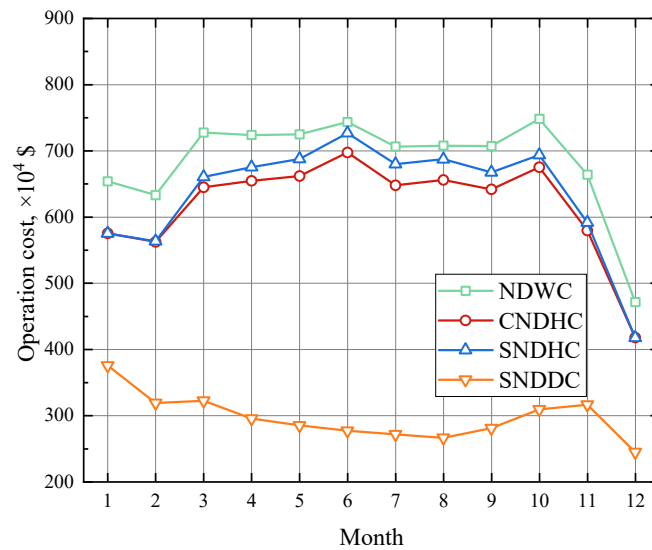


Figure 14. The operating costs of different cooling systems in Yangcheng.

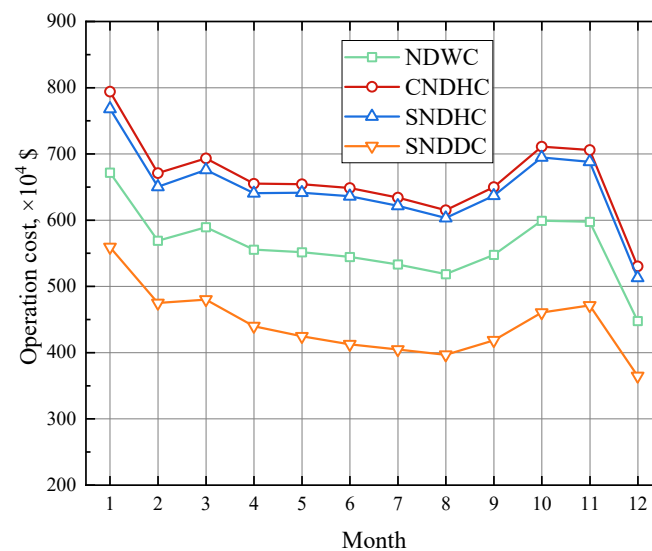


Figure 15. The operating costs of different cooling systems in Lianjiang.

To further explore optimization directions, the total operating costs are broken down into pump operation costs and makeup water costs, as shown in Figure 16. The left chart represents the Yangcheng plant, while the right chart represents the Lianjiang plant. It can be observed that compared to NDWC, NDHC has lower makeup water costs but higher pump operation costs. In the climate of Yangcheng, NDHC has a higher proportion of makeup water costs, and only in colder months are makeup water costs lower than pump operation costs. In the climate conditions of Lianjiang, it was found that the pump operation costs of the CNDHC exceeded makeup water costs. For the SNDHC, in colder months, pump operation costs are higher, while in hot summers, makeup water costs are higher. SNDDC has the highest pump operation costs due to it having the largest number of pumps.

This indicates that the proportion of pump operation costs cannot be ignored. Subsequent optimization can be achieved by adjusting the ratio of circulating water entering the dry and wet sections to reduce the pump operation consumption and evaporative losses of circulating water. This is expected to expand the applicability of hybrid systems further.

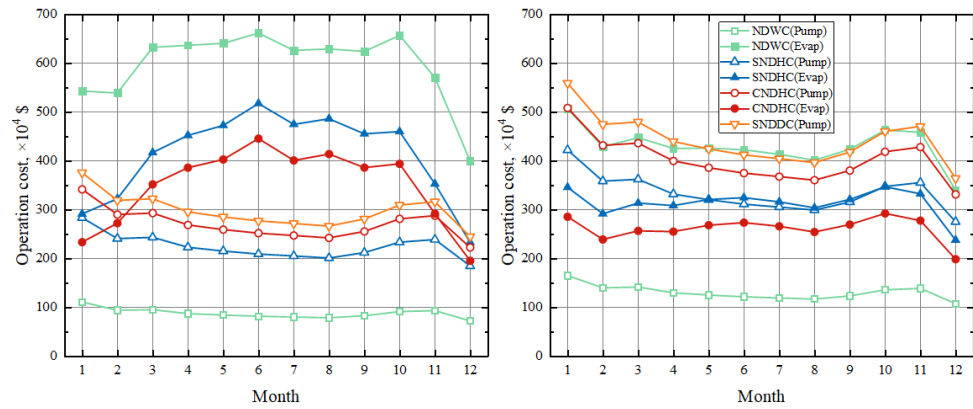


Figure 16. The operating costs of different cooling systems ((left): Yangcheng, (right): Lianjiang).

4.6. Net Benefit

The formula for calculating the net profit is as follows:

$$E = W \times t \tag{54}$$

$$Profit = E \times C_{eav} - C_{tot} \tag{55}$$

$$Profit_h = Profit / t \tag{56}$$

where E represents the total revenue, CNY; W represents the power generation capacity, kW; t represents the operating time, h; C_{eav} represents the on-grid electricity price, CNY/kWh; C_{tot} represents the annual average cost, CNY/annum; $Profit$ represents the total net profit, CNY; and $Profit_h$ represents the hourly net profit, CNY/hour.

The annual average cost of different cooling systems includes the following three components: tower construction annual amortization, operating cost, and maintenance cost. Table 13 presents the tower construction annual amortization for each cooling system. NDWC has the lowest cost due to its single and small tower design, followed by CNDHC. SNDHC and SNDDC, due to their double-tower design, occupy a larger space, resulting in higher tower construction costs, which are higher than that of single-tower systems.

Table 13. Tower construction annual amortization.

Capital Cost ($\times 10^4$ CNY/Annum)	Value
NDWC	2000
CNDHC	3395
SNDHC	1640 (NDWC)/2232 (NDDC)
SNDDC	2248 \times 2

Choosing SNDDC as the baseline with zero net profit, the chart in Figure 17 illustrates the monthly variation in net profit for different cooling systems in Yangcheng. From this graph, it can be observed that the higher the temperature, the more pronounced the advantage in net profit for NDWC, reaching the maximum difference with CNDHC in June. As mentioned earlier, NDWC, lacking a dry section for heat exchange, relies solely on the evaporative cooling of circulating water in the fill, resulting in the maximum evaporative loss and, subsequently, the highest operating cost. However, as the temperature rises, the gap in operating costs between NDWC and the hybrid system narrows. The non-standardized multiple linear regression curve on evaporative loss in Section 4.1 indicates that the coefficient of T_a for NDWC is as high as 17.86, surpassing the dry-bulb temperature coefficients of 8.56 for CNDHC and 2.99 for SNDHC. Therefore, with increasing temperatures, the advantage of the combined system in operating costs diminishes. Furthermore, coupling the nuclear power generation system with the wet-cooling tower in June, when the power output of the CNDHC power generation system is at its highest and that of the NDWC system is at its lowest throughout the year, leads to the peak net profit for NDWC in June, with the maximum difference from the combined system’s net profit.

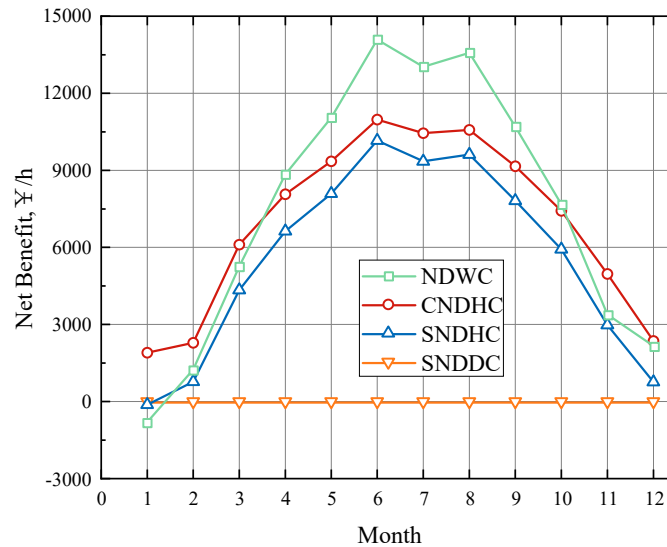


Figure 17. Monthly variations in the net benefit for different cooling systems in Yangcheng.

When the temperature decreases, the profits of the hybrid cooling system and SNDDC gradually surpass NDWC. This is because, in colder months, NDWC has the highest back pressure, lowest power output, and the highest operating costs, resulting in the lowest net profit for the wet-cooling tower in January. The slopes of the curves also indicate that the net profit of NDWC is most sensitive to environmental changes. The hybrid system shows better adaptability to environmental variations, and CNDHC outperforms SNDHC. Calculating the total annual net profit for 2018, it was found that CNDHC is only CNY 48,000 lower than NDWC, which is negligible in the context of the project.

Although SNDDC has the lowest operating costs, its highest tower construction cost and back pressure result in the worst economic performance.

The chart in Figure 18 illustrates the monthly net profits of different cooling systems in Lianjiang. In the humid climate of the south, lower operating costs keep NDWC's net profit consistently at the highest. The two-hybrid cooling systems, with similar power generation and operating costs, have a small difference in net profit. SNDDC, due to its less apparent water-saving advantage in a humid climate, exhibits a significant gap in net profit compared to other cooling systems.

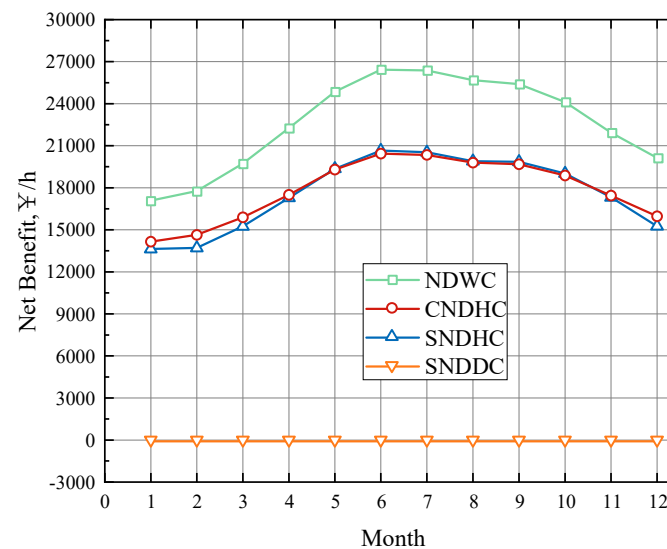


Figure 18. Monthly variations in the net benefit for different cooling systems in Lianjiang.

5. Conclusions

This study developed a numerical simulation model for NDHC, referencing meteorological data from typical years in different locations. This model was coupled with the cooling system and the nuclear power generation unit to explore the environmental adaptability of inland nuclear power plant cooling systems. The simulation results for the operating parameters of different cooling systems were obtained, and economic analysis and comparison of the cooling systems were conducted. The conclusions are as follows:

- (1) When the dry-bulb temperature changes by 1 °C, the variation in the evaporation rate of NDWC is 17.86 kg/s and SNDHC changes by 2.99 kg/s.
- (2) Compared to NDWC, SNDHC exhibits a monthly average cycle water evaporation rate that is reduced by 190 kg/s, while CNDHC shows a reduction of 270 kg/s.
- (3) In the case study, the back pressure of NDHC is close to that of NDWC but is more than 5 kPa and lower than that of SNDHC.
- (4) In the dry and water-deficient region, the average monthly operating cost of SNDHC is CNY 480,000 lower than that of NDWC, and the operating cost of CNDHC is CNY 660,000 lower than that of NDWC.
- (5) In arid regions, the annual net profit of NDWC is only CNY 48,000 higher than that of CNDHC. However, the net profit curve of CNDHC is more stable, with less susceptibility to environmental changes. CNDHC demonstrates the best environmental adaptability.

6. Discussion

As anticipated, compared to traditional cooling systems, Natural Draft Hybrid Cooling Towers (NDHCs) exhibit stronger resilience to environmental factors in terms of their cooling performance and economic efficiency, granting them broader environmental adaptability. However, the current high tower structure and significant initial investment costs of NDHC have become limiting factors for their development. Maintaining a consistent back pressure while minimizing investment and operating costs is a key focus of future research. To enhance the net profit of NDHC and expand the applicability of hybrid systems, we propose the following plans:

- (1) **Structural Design and Simulation:** Design and simulate more NDHC structures, such as adding wet cooling filling sections inside indirect dry cooling towers, replacing the natural draft with a mechanical draft, and designing the tower as a cylinder–cone combination instead of a hyperbolic shape. These different designs can be compared in terms of heat transfer performance and economic efficiency.
- (2) **Parameter Optimization:** Optimize the tower parameters to reduce the tower structure while maintaining the same heat transfer capacity, thereby reducing investment costs and footprint.
- (3) **Water Distribution:** The current NDHC in this study operates with a series of water distributions. Future work should explore parallel water distribution for the dry and wet sections and optimize the water distribution ratio.

Author Contributions: Conceptualization, H.W.; Methodology, W.Z.; Validation, Y.L.; Formal analysis, P.L.; Data curation, Y.L.; Writing—original draft, W.Z.; Writing—review & editing, H.W. All authors have read and agreed to the published version of the manuscript.

Funding: The financial support for this research project came from China National Natural Science Foundation (No. 52006066).

Data Availability Statement: The original contributions presented in the study are included in the article, further inquiries can be directed to the corresponding author.

Conflicts of Interest: Authors Wenjie Zhang and Yushan Li were employed by the China Nuclear Power Engineering Co., Ltd. The remaining authors declare that the research was conducted in the absence of any commercial or financial relationships that could be construed as a potential conflict of interest.

Nomenclature

A	area (m ²)
c_p	specific heat (J kg ⁻¹ K ⁻¹)
d	diameter (m)
ex	exergy rate (W)
F_M	correction factor for the material of condenser
F_C	correction factor for the wall thickness of condenser
F_T	correction factor for counterflow logarithmic mean temperature difference
Fr_D	densimetric Froude number
g	gravitational acceleration (m s ⁻²)
h	heat transfer coefficient (W m ⁻² K ⁻¹)/height (m)/enthalpy (J/kg)
k	flow loss coefficient
L	length (m)
m	mass flow rate (kg s ⁻¹)
M	mass flow rate of steam (kg s ⁻¹)
Me	Merkel number
p	pressure (Pa)
Pr	Prantl number
q	heat output of extraction steam (J/kg)
Q	heat flux (W m ⁻²)
Re	Reynolds number
T	temperature (K)
v	velocity magnitude (m s ⁻¹)
<i>Greek symbols</i>	
ε	effectiveness
ρ	density (kg m ⁻³)
ζ	lapse rate for pseudo-adiabatic process (K m ⁻¹)
η	efficiency
τ	enthalpy rise of feed water (J/kg)
γ	heat output of drainage water (J/kg)
<i>Subscripts</i>	
1, 2, ..., 10	positions within or around the towers
a	air/ambient
av	air vapor
b	bundle
ct	cooling tower
ctc	cooling tower contraction
cte	cooling tower expansion
d	dry/drainage water
es	extraction steam
fi	fill
fw	feed water
fr	frontal
he	heat exchanger
i	ith stage group
j	jth extraction
in	inlet
out	outlet
m	mean
ms	main steam
reh	reheater
rz	rain zone
sp	spray
std	standard
tb	tubes per bundle
t	tower/tube
tot	total

w	water/wet
wi	water inlet
wo	water outlet
r_n	polynomial coefficient of non-dimensional loss coefficient
v	velocity magnitude (m s^{-1})

References

- He, S.; Gurgenci, H.; Guan, Z.; Huang, X.; Lucas, M. A review of wetted media with potential application in the pre-cooling of natural draft dry cooling towers. *Renew. Sustain. Energy Rev.* **2015**, *44*, 407–422. [\[CrossRef\]](#)
- Wei, H.; Wu, T.; Ge, Z.; Yang, L.; Du, X. Entransy analysis optimization of cooling water flow distribution in a dry cooling tower of power plant under summer crosswinds. *Energy* **2019**, *166*, 1229–1240. [\[CrossRef\]](#)
- Wu, X.P.; Yang, L.J.; Du, X.Z.; Yang, Y.P. Flow and heat transfer characteristics of indirect dry cooling system with horizontal heat exchanger A-frames at ambient winds. *Int. J. Therm. Sci.* **2014**, *79*, 161–175. [\[CrossRef\]](#)
- Du Preez, A.F.; Kröger, D.G. The effect of the heat exchanger arrangement and wind-break walls on the performance of natural draft dry-cooling towers subjected to cross-winds. *J. Wind. Eng. Ind. Aerodyn.* **1995**, *58*, 293–303. [\[CrossRef\]](#)
- Su, M.D.; Tang, G.F.; Fu, S. Numerical simulation of fluid flow and thermal performance of a dry-cooling tower under cross wind condition. *J. Wind. Eng. Ind. Aerodyn.* **1999**, *79*, 289–306. [\[CrossRef\]](#)
- Wang, W.; Wang, Y.; Zhang, H.; Lin, G.; Lu, J.; Yue, G.; Ni, W. Fresh breeze cuts down one-third ventilation rate of a natural draft dry cooling tower: A hot state modelling. *Appl. Therm. Eng.* **2018**, *131*, 1–7. [\[CrossRef\]](#)
- Wang, W.; Lv, J.; Zhang, H.; Liu, Q.; Yue, G.; Ni, W. A quantitative approach identifies the critical flow characteristics in a natural draft dry cooling tower. *Appl. Therm. Eng.* **2018**, *131*, 522–530. [\[CrossRef\]](#)
- Wang, W.; Yang, L.; Du, X.; Yang, Y. Anti-freezing water flow rates of various sectors for natural draft dry cooling system under wind conditions. *Int. J. Heat Mass Transf.* **2016**, *102*, 186–200. [\[CrossRef\]](#)
- He, S.; Gurgenci, H.; Guan, Z.; Hooman, K.; Zou, Z.; Sun, F. Comparative study on the performance of natural draft dry, pre-cooled and wet cooling towers. *Appl. Therm. Eng.* **2016**, *99*, 103–113. [\[CrossRef\]](#)
- He, S.; Guan, Z.; Gurgenci, H.; Hooman, K.; Lu, Y.; Alkhedhair, A.M. Experimental study of the application of two trickle media for inlet air pre-cooling of natural draft dry cooling towers. *Energy Convers. Manag.* **2015**, *89*, 644–654. [\[CrossRef\]](#)
- Sun, Y.; Guan, Z.; Gurgenci, H.; Wang, J.; Dong, P.; Hooman, K. Spray cooling system design and optimization for cooling performance enhancement of natural draft dry cooling tower in concentrated solar power plants. *Energy* **2019**, *168*, 273–284. [\[CrossRef\]](#)
- Patankar, S.V. *Numerical Heat Transfer and Fluid Flow*; Hemisphere Series on Computational Methods in Mechanics and Thermal Science; Hemisphere Publishing Corporation (CRC Press, Taylor & Francis Group): Boca Raton, FL, USA, 1980.
- Zhou, X.; Wang, W.; Chen, L.; Yang, L.; Du, X. Numerical investigation on novel water distribution for natural draft wet cooling tower. *Int. J. Heat Mass Transf.* **2021**, *181*, 121886. [\[CrossRef\]](#)
- Merkel, F. *Verdunstungskühlung*; VDI-Verlag: Berlin, Germany, 1925.
- Poppe, M.; Rögener, H. Berechnung von rückkühlwerken. *VDI-Wärmeatlas* **1991**, *111*, 1–15.
- Kloppers, J.C. A Critical Evaluation and Refinement of the Performance Prediction of Wet-Cooling Towers. Ph.D. Thesis, University of Stellenbosch, Stellenbosch, South Africa, 2003.
- Williamson, N.J. *Numerical Modelling of Heat and Mass Transfer and Optimisation of a Natural Draft Wet Cooling Tower*; The University of Sydney: Sydney, Australia, 2008.
- Al-Waked, R. Crosswinds effect on the performance of natural draft wet cooling towers. *Int. J. Therm. Sci.* **2010**, *49*, 218–224. [\[CrossRef\]](#)
- Al-Waked, R.; Behnia, M. CFD simulation of wet cooling towers. *Appl. Therm. Eng.* **2006**, *26*, 382–395. [\[CrossRef\]](#)
- Al-Waked, R.; Behnia, M. Enhancing performance of wet cooling towers. *Energy Convers. Manag.* **2007**, *48*, 2638–2648. [\[CrossRef\]](#)
- Xia, L.; Li, J.; Ma, W.; Gurgenci, H.; Guan, Z.; Wang, P. Water Consumption Comparison Between a Natural Draft Wet Cooling Tower and a Natural Draft Hybrid Cooling Tower—An Annual Simulation for Luoyang Conditions. *Heat Transf. Eng.* **2017**, *38*, 1034–1043. [\[CrossRef\]](#)
- Huang, Y.; Chen, L.; Huang, X.; Du, X.; Yang, L. Performance of natural draft hybrid cooling system of large scale steam turbine generator unit. *Appl. Therm. Eng.* **2017**, *122*, 227–244. [\[CrossRef\]](#)
- Chen, L.; Peng, X.; Huang, Y.; Yang, L.; Du, X.; Yang, Y. Performance analysis of hybrid cooling tower based on effectiveness-NTU method. *J. Eng. Thermophys.* **2018**, *39*, 144–149.
- Wei, H.; Huang, X.; Chen, L.; Yang, L.; Du, X. Performance prediction and cost-effectiveness analysis of a novel natural draft hybrid cooling system for power plants. *Appl. Energy* **2020**, *262*, 114555. [\[CrossRef\]](#)
- Huang, Q.; Zhi, Y.; Zhang, R.; Wei, H.; Xu, L. Comprehensive Comparison of Hybrid Cooling of Thermal Power Generation with Airside Serial and Parallel Heat Exchange. *Energies* **2022**, *15*, 6478. [\[CrossRef\]](#)
- Welty, J.; Rorrer, G.L.; Foster, D.G. *Fundamentals of Momentum, Heat, and Mass Transfer*; John Wiley & Sons: Hoboken, NJ, USA, 2014.
- Turgut, O.E.; Asker, M.; Coban, M.T. A review of non iterative friction factor correlations for the calculation of pressure drop in pipes. *Bitlis Eren Univ. J. Sci. Technol.* **2014**, *4*, 1–8. [\[CrossRef\]](#)

28. Thomas, L.C. *Fundamentals of Heat Transfer*; Prentice-Hall: Hoboken, NJ, USA, 1980.
29. Wei, H.; Chen, L.; Ge, Z.; Yang, L.; Du, X. Influence of Operation Schemes on the Performance of the Natural Draft Hybrid Cooling System for Thermal Power Generation. *Energies* **2021**, *14*, 5653. [[CrossRef](#)]
30. De Villiers, E.; Kröger, D.G. Analysis of heat, mass, and momentum transfer in the rain zone of counterflow cooling towers. *J. Eng. Gas Turbines Power* **1999**, *121*, 751–755. [[CrossRef](#)]
31. Kröger, D.G. *Air-Cooled Heat Exchangers and Cooling Towers*; Penwell Corporation Oklahoma: Tulsa, OK, USA, 2004; Volume 1.
32. Hensley, J.C. *Cooling Tower Fundamentals*; Marley Cooling Tower Company: Stockton, CA, USA, 1985.
33. Harpster, T.J.; Harpster, J.W. Instrumentation for the Advancement of Shell and Tube Heat Exchanger Design or for Implementing an Upgrade via a Retrofit Process. In Proceedings of the ASME Power Conference, Charlotte, NC, USA, 26–30 June 2017; American Society of Mechanical Engineers: New York, NY, USA, 2017; Volume 57601, p. V001T05A015.
34. Zhang, C. Proof for part of the Sttla flow experimental conclusion and the improvement of Flugel formula. *Sci. China Ser. E* **2002**, *45*, 35. [[CrossRef](#)]
35. Conradie, A.E. Performance Optimization of Engineering Systems with Particular Reference to Dry-Cooled Power Plants. Ph.D. Thesis, University of Stellenbosch, Stellenbosch, South Africa, 1995.
36. Kloppers, J.C.; Kröger, D.G. Cost optimization of cooling tower geometry. *Eng. Optim.* **2004**, *36*, 575–584. [[CrossRef](#)]
37. Jingyu, C.; Wuquan, L.; Jingwei, Z. Research on applying dry cooling technology in conventional island of ap1000 nuclear power in China. In Proceedings of the 17th IAHR International Conference on Cooling Tower and Heat Exchanger, Gold Coast, QLD, Australia, 7–11 September 2015; pp. 101–108.
38. Rezaei, E.; Shafiei, S.; Abdollahnezhad, A. Reducing water consumption of an industrial plant cooling unit using hybrid cooling tower. *Energy Convers. Manag.* **2010**, *51*, 311–319. [[CrossRef](#)]
39. Asvapoositkul, W.; Kuansathan, M. Comparative evaluation of hybrid (dry/wet) cooling tower performance. *Appl. Therm. Eng.* **2014**, *71*, 83–93. [[CrossRef](#)]
40. Barigozzi, G.; Perdichizzi, A.; Ravelli, S. Wet and dry cooling systems optimization applied to a modern waste-to-energy cogeneration heat and power plant. *Appl. Energy* **2011**, *88*, 1366–1376. [[CrossRef](#)]

Disclaimer/Publisher’s Note: The statements, opinions and data contained in all publications are solely those of the individual author(s) and contributor(s) and not of MDPI and/or the editor(s). MDPI and/or the editor(s) disclaim responsibility for any injury to people or property resulting from any ideas, methods, instructions or products referred to in the content.